

This is an electronic reprint of the original article. This reprint may differ from the original in pagination and typographic detail.

Rapid Quenching of Molten Salts as an Approach for the Coordination Characterization of Corrosion Products

Lehmusto, Juho; Kurley III, J. Matthew; Cakmak, Ercan; Keiser, James R.; Lindberg, Daniel; Engblom, Markus; Pint, Bruce A.; Raiman, Stephen S.

Published in:
Nuclear Science and Engineering

DOI:
<https://doi.org/10.1080/00295639.2023.2204175>

Published: 15/05/2023

Document Version
Final published version

Document License
CC BY

[Link to publication](#)

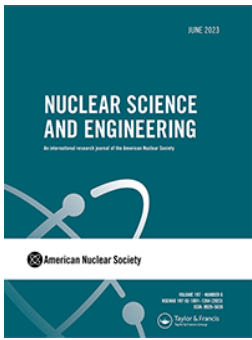
Please cite the original version:
Lehmusto, J., Kurley III, J. M., Cakmak, E., Keiser, J. R., Lindberg, D., Engblom, M., Pint, B. A., & Raiman, S. S. (2023). Rapid Quenching of Molten Salts as an Approach for the Coordination Characterization of Corrosion Products. *Nuclear Science and Engineering*. <https://doi.org/10.1080/00295639.2023.2204175>

General rights

Copyright and moral rights for the publications made accessible in the public portal are retained by the authors and/or other copyright owners and it is a condition of accessing publications that users recognise and abide by the legal requirements associated with these rights.

Take down policy

If you believe that this document breaches copyright please contact us providing details, and we will remove access to the work immediately and investigate your claim.



Rapid Quenching of Molten Salts as an Approach for the Coordination Characterization of Corrosion Products

Juho Lehmusto, J. Matthew Kurley III, Ercan Cakmak, James R. Keiser, Daniel Lindberg, Markus Engblom, Bruce A. Pint & Stephen S. Raiman

To cite this article: Juho Lehmusto, J. Matthew Kurley III, Ercan Cakmak, James R. Keiser, Daniel Lindberg, Markus Engblom, Bruce A. Pint & Stephen S. Raiman (2023): Rapid Quenching of Molten Salts as an Approach for the Coordination Characterization of Corrosion Products, Nuclear Science and Engineering, DOI: [10.1080/00295639.2023.2204175](https://doi.org/10.1080/00295639.2023.2204175)

To link to this article: <https://doi.org/10.1080/00295639.2023.2204175>



© 2023 The Author(s). Published with license by Taylor & Francis Group, LLC.



Published online: 15 May 2023.



Submit your article to this journal [↗](#)



Article views: 59



View related articles [↗](#)



View Crossmark data [↗](#)



Rapid Quenching of Molten Salts as an Approach for the Coordination Characterization of Corrosion Products

Juho Lehmusto,^{id a*} J. Matthew Kurley III,^{id b} Ercan Cakmak,^{id c} James R. Keiser,^{id c} Daniel Lindberg,^{id d} Markus Engblom,^{id a} Bruce A. Pint,^{id c} and Stephen S. Raiman^{id e}

^a*Abo Akademi University, Faculty of Science and Engineering, Turku, Finland*

^b*Oak Ridge National Laboratory, Nuclear Energy and Fuel Cycle Division, Oak Ridge, Tennessee*

^c*Oak Ridge National Laboratory, Materials Science and Technology Division, Oak Ridge, Tennessee*

^d*Aalto University, Department of Chemical and Metallurgical Engineering, Espoo, Finland*

^e*University of Michigan, Nuclear Engineering & Radiological Sciences, Ann Arbor, Michigan*

Received December 8, 2022

Accepted for Publication April 14, 2023

Abstract — *A new apparatus was built to rapidly cool molten salts in liquid argon to prevent contamination during quenching and enable new insight into the structure in the liquid state. To test the applicability of the apparatus, several industrially relevant chloride salt compositions were first melted, rapidly solidified, and then characterized. The design proved applicable for the rapid quenching of molten salt. Furthermore, the structure of the apparatus prevented exposure of the rapidly quenched salt to impurities (humidity, oxygen, etc.). X-ray diffraction of salt specimens cooled with and without liquid argon showed differences including a structure further from the expected stoichiometric equilibrium with rapid cooling. Of particular interest is the chemical state of metallic impurities, and this may be probed using electron paramagnetic resonance.*

Keywords — *Molten chlorides, solidification process, high-temperature corrosion, crystal structure.*

Note — *Some figures may be in color only in the electronic version.*

I. INTRODUCTION

Molten salts might play an important role in power production, where they can be used as a thermal energy storage medium or as a heat transfer fluid in concentrating solar power (CSP) plants or for molten salt reactors.^[1] Current state-of-the-art CSP plants operate

below 600°C, using nitrate salts for heat transfer and thermal storage. However, to make solar electricity cost-competitive with power from conventional generation technologies, CSP plants will need to operate at higher temperatures. Currently, the thermal properties and stability of molten salts together with a possibly detrimental interaction between the melt and structural materials limit the operating temperatures and, thus, efficiencies of the applications.

Because of their thermal stability, chloride salts are a candidate to replace nitrate salts at >600°C.^[2] Most chloride salts also have a low vapor pressure up to 801°C and are projected to lower the cost of electricity.^[3,4] In addition, although displaying poorer heat transfer performance, the raw material costs of

*E-mail: juho.lehmusto@abo.fi

This is an Open Access article distributed under the terms of the Creative Commons Attribution License (<http://creativecommons.org/licenses/by/4.0/>), which permits unrestricted use, distribution, and reproduction in any medium, provided the original work is properly cited. The terms on which this article has been published allow the posting of the Accepted Manuscript in a repository by the author(s) or with their consent.

chloride salts are significantly lower than those of other higher-temperature salts such as fluorides, fluoroborates, and lithium-containing salts.^[5]

A major challenge with the use of chloride salts is their corrosivity at higher temperatures in the presence of oxygen-containing species such as air or water, which might exist as dissolved impurities in the molten phase.^[6,7] Humidity requires particular attention as most of the chloride salts are hygroscopic and moisture-based impurities are known to accelerate corrosion. Especially chromium-containing alloys are susceptible to selective leaching of active constituents due to the higher solubility of chromium oxide (Cr_2O_3) compared with the solubilities of nickel and iron oxides.^[8] A correlation between the salt impurity level and the attack of structural alloys has been demonstrated.^[9,10]

To better understand the role of molten salts and their impurities on corrosion, including developing salt purity standards, more information on the salts themselves is required. Unfortunately, analysis and characterization of molten salts at temperature are technically challenging, limiting the number of suitable techniques available. Therefore, an approach allowing studies on solid salts, which would still provide information related to the molten phase, would tremendously widen the possibilities in terms of characterization techniques. To capture the structure at high temperature in the solid phase, molten salts have been solidified (1) by a melt spinning method,^[11] (2) by immersion and removal of a tungsten rod,^[12] and (3) by dumping the molten salt on a steel plate.^[13] However, it might be possible to further increase cooling rates compared to these techniques.

Cryogenic liquids are one alternative for quenching. The mode of heat transfer depends on the temperature difference between the bulk liquid and the object to be quenched. With a hot object, the low boiling point of the liquid results in the formation of a vapor film at the interface between the object and the bulk liquid.^[14,15] The vapor film has an insulating effect and lowers the cooling rate compared to the situation of the bulk fluid in direct contact with the object to be cooled. The cooling rate also depends on the size of the object. For spheres, a smaller diameter results in higher cooling rates. Relevant to the present work, Xu and Zhang studied the quenching of hydrous rhyolite in different media.^[16] They found that in liquid nitrogen, the quench rates for millimeter-sized objects are about 200 K/s. Xu and Zhang also determined for their samples a so-called apparent equilibrium temperature, which characterizes the temperature at which the object's chemical composition has effectively frozen during the quench. For the millimeter-

sized sample in liquid nitrogen, the Xu and Zhang apparent equilibrium temperatures are about 700°C. The exact initial temperatures for each sample are not given, but samples, in general, are reported to have been heated to an initial temperature between 720°C to 750°C.

While quenching media other than cryogenic liquids could provide faster cooling rates, it is imperative that the solidification technique applied for salt structure studies be operated in an environment without the risk of contamination in order to isolate impurities. For that, this paper presents a novel design to quench molten salts extremely rapidly in an inert environment. It is hypothesized that accelerating the quenching process will reduce the time available for the structure to reorganize, thus preserving information relevant to the molten phase. The technique was demonstrated on molten chloride mixtures, and the crystal structures and bonding characteristics were studied after solidification.

II. EXPERIMENTAL

The principle of the designed reactor is to melt salt and then solidify it rapidly in a bath of liquid argon, all in a well-controlled manner without contamination. The reactor consisted of two larger sections, i.e., the lid and the round-bottomed body, both made of quartz glass (Fig. 1a). There is an O-ring at the upper end of the body to precisely seal the body to the lid, which is kept in position with a horseshoe clamp. In the upper part of the body, there is an inlet tube for the dried argon gas and a large outlet tube to safely vent argon gas and prevent pressure buildup. For operation, the inlet was connected to an argon cylinder, and during the exposure, the reactor was flushed with gaseous argon to sustain the protective atmosphere. From the outlet, a tube was led to an oil-filled bubbler that indicated that the reactor was airtight and that the gas was flowing in the desired direction through the reactor. The reactor body was positioned in a vacuum-insulated container, and before introducing liquid argon, the body was cooled from the outside with liquid nitrogen. Liquid nitrogen was used to provide cooling beyond the capability of liquid argon. During initial cooling with liquid nitrogen, the flow of gaseous argon was adjusted to prevent backflow from the oil bubbler.

The lid consisted of an inlet tube for liquid argon, an ~15-cm-deep thermal well, and an ~23-cm-long vertical tube for the sample holder and thermocouple. Another port was located outside of the thermal well to introduce liquid argon from a pressurized container with a copper

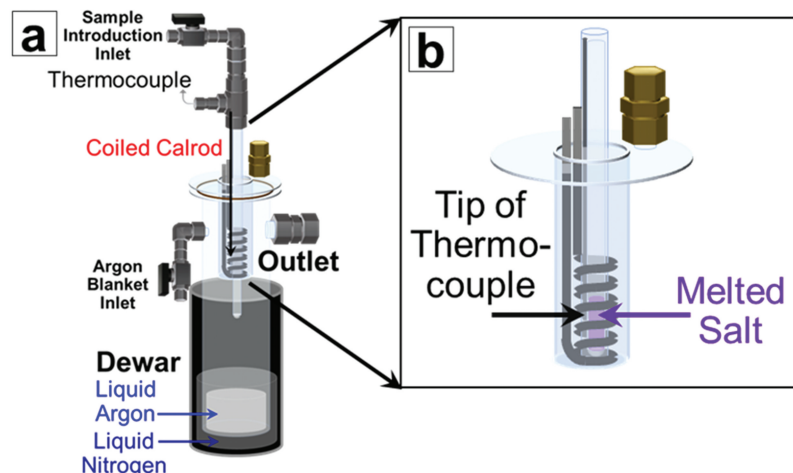


Fig. 1. (a) Schematic of the Rapid Quenching Reactor with (b) magnification of the sample holder.

tube. A coiled heating element was located around the vertical tube at the bottom of the thermal well (Fig. 1b). The coils were evenly distributed to ensure a homogeneous temperature profile during heating. With the thermocouple inside the vertical tube, the temperature of the coil was constantly monitored and adjusted as necessary. The sample holder was a round-bottomed quartz tube with an orifice in the middle of its bottom. The sample tube was loaded in an inert glove box and sealed using an O-ring sealed valve and cap. The sample introduction inlet gas line was attached while flowing argon to maintain an air-free environment. The salt sample was positioned at the bottom of the sample holder and heated above the melting temperature. Once the sample was completely molten, a very small argon flow was introduced from the top of the sample holder, forcing the molten sample through the orifice into the liquid argon. The cooling rate of the molten sample was not calculated, but based on a study with a similar cooling medium (liquid nitrogen), the cooling rate is on the order of $200^{\circ}\text{C}/\text{s}$, but the apparent equilibrium temperature will be reached much faster.^[16] When the sample introduction was complete, the reactor was left standing to allow the liquid argon to slowly boil off while maintaining an air-free environment. After the evaporation of the liquid argon, the reactor was sealed and taken to the glove box for sample removal.

As a demonstration, a pre-purified $\text{NaCl}:\text{MgCl}_2$ (58:42) mixture was melted and cooled by splat quenching (lower cooling rate) and with the novel design (faster cooling rate). The salt was prepared and purified utilizing a two-step carbochlorination procedure.^[9] Briefly, as-delivered MgCl_2 was first dehydrated by melting in the presence of ammonium chloride in an Ar stream passing

over P_2O_5 to remove moisture. Then, the fused salt mixture was purified with CCl_4 to remove oxide impurities, which would react with the CCl_4 , forming CO . The impurity (MgO) content of such high-purity salt has been reported to be $50 \mu\text{mol}\cdot\text{kg}^{-1}$.^[9] Further details on the purity analyses, in addition to the salt preparation procedure, can be found in reference.^[9] The produced salt mixture was kept in a sealed glove box under argon to avoid contamination from the surroundings. For splat quenching, a stainless steel plate was positioned at the bottom of the same reactor, and the molten sample was dropped onto the plate instead of into a bath of liquid argon. Experiments were performed with a purified $\text{KCl}:\text{MgCl}_2$ (68:32) mixture. Additionally, a batch of the $\text{KCl}:\text{MgCl}_2$ (68:32) salt was mixed with 5 wt% CrCl_3 to study the speciation of Cr in the melt. To produce a third melt with 5 wt% CrCl_2 , the CrCl_3 mixture was sparged with $\text{Ar} + 4\% \text{H}_2$ overnight. Four percent of H_2 is enough to reduce CrCl_3 to CrCl_2 , but any traces of oxygen will most likely stay with Cr. However, what should be noticed is the low amount of oxygen relative to Cr: Even with 100 ppm O_2 (worst-case scenario), 1.3 mmol O would yield over the course of the reduction (at most). The introduced molten salt sample contained roughly 50 mmol CrCl_3 , so even if all of the oxygen was captured, it would be only about 2% relative to Cr. With 5 mol% Cr in the salt, that would be 0.1% CrO_x species, which is well below detection limits in a benchtop X-ray powder diffraction (XRD).

Both studied mixtures ($\text{NaCl}:\text{MgCl}_2$ and $\text{KCl}:\text{MgCl}_2$) are more stable under these conditions than metal chlorides, which might form in a reaction between the structural material and molten salt (Fig. 2). The fact that the major salt components are more stable

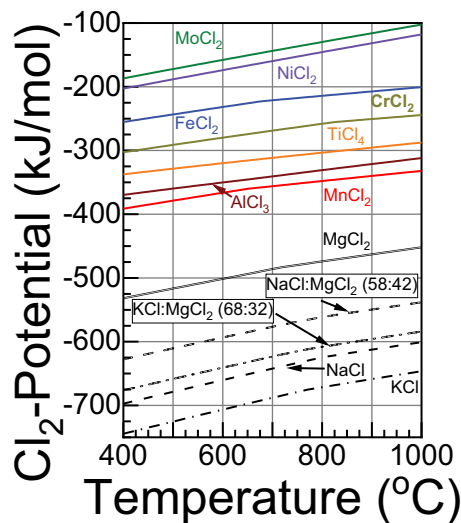


Fig. 2. Chlorine potential of various chlorides calculated as a function of temperature.

originates from their more negative Gibbs free energy of formation compared to those of the metal chlorides, which might form through corrosion. In other words, the studied salt mixtures are lower than the corrosion products on the Ellingham diagram presented in Fig. 2. When studying the mixtures, the samples were heated in argon up to 200°C above the melting temperature of the studied mixture and kept there until the entire sample was molten. After this, the molten sample was introduced into liquid argon or onto a cooled steel plate to be solidified instantaneously. The melting points of the studied mixtures are 430°C for NaCl:MgCl₂,^[17] 426°C for KCl:MgCl₂,^[18,19] and 422°C for KCl:MgCl₂+CrCl₃. The melting behavior of the KCl:MgCl₂+CrCl₃ was calculated using the thermodynamic software package FactSage, version 8.2.^[20] The thermodynamic data used for the calculations were taken from the Fact Pure Substance (FactPS) database for stoichiometric compounds, as well as from the FTSalt database and the publication by Ard et al.,^[21] as the FTSalt database does not include data for CrCl₃. More specifically, the thermodynamic interaction parameters for the liquid phase in the binary systems that form the basis for the calculations of ternary mixtures are taken from Pelton and Chartrand (NaCl:MgCl₂; KCl:MgCl₂)^[22] and Ard et al. (KCl:CrCl₃; MgCl₂:CrCl₃).^[21] It should be noted that the thermodynamic model of Chartrand and Pelton did not consider the formation of Na₆MgCl₈ either due to absence of the phase in previous studies or lack of consistent thermodynamic data in the sources they used as input. However, Seifert and Thiel^[23] have measured the thermodynamic properties of the compound,

and their reported experimental phase diagram suggests similar melting behavior compared to Na₂MgCl₄.

For the studied KCl:MgCl₂+CrCl₃ system, the predicted solidus temperature or first melting temperature T_0 is predicted to be 422°C, and the predicted liquidus temperature is 619°C. To our knowledge, no reported phase equilibrium measurements have been done for this ternary system.

After quenching by the previously described methods, the solidified samples were characterized by XRD to study the crystal structure. Continuous θ -2 θ scans were performed on the Panalytical X'pert diffractometer from nominally 5 to 90 deg 2 θ using CuK α radiation ($\lambda = 1.540598 \text{ \AA}$). All scans used 1/4-deg fixed slits, 1/2-deg anti-scatter slit, 0.04 soller slits coupled with a 10-mm mask (beam length). For the phase identification procedure, a search match was conducted using Jade software^[24] and the ICDD database.^[25]

In addition, electron paramagnetic resonance (EPR) using an Elexsys E580 from Bruker was utilized with the Cr-containing mixtures to identify the oxidation states and speciation of chromium in the solidified sample.

III. RESULTS AND DISCUSSION

III.A. Reactor Operation

Depending on the introduced argon flow through the sample holder, spherical pieces of salt with varying diameters (1 to 5 mm) were solidified in liquid argon. The solidification of the molten sample with the new design can be considered controllable whereas samples produced by splat quenching did not have a uniform size or shape. Also, the reactor did not have any issues with glass cracking or pressure increases during the experiments. The small flow of dry argon through the bottom part of the reactor during the experiments successfully prevented air leakage, thus eliminating the risk of contamination. The transparent quartz glass allowed easy monitoring and adjustment of the melting process. The coiled design of the heating element provided homogeneous heat transfer.

Although not the focus of the current study, it was verified that by adjusting the argon flow, the size of the solidified salt could be regulated. Similarly, although not addressed in the current study, the Rapid Quenching Reactor could be applicable to studies of viscosity and surface tension of molten phases in addition to the rapid solidification of molten salts. The viscosity studies could be carried out with a high enough underpressure in the sample holder to keep the molten salt in position. Then,

the pressure would be increased in a precisely controlled manner and recorded at the point when the molten salt is able to escape the sample holder through the orifice.

III.B. X-Ray Powder Diffraction

Based on the starting composition, the stoichiometric composition of the studied NaCl:MgCl₂ mixture when molten was calculated to be NaMgCl₃ (92%) and Na₆MgCl₈ (8%), giving a NaMgCl₃-to-Na₆MgCl₈ ratio of 12.1. This ratio was 8.2 for splat quenching but dropped to 0.4 with the rapid-quenched samples, respectively (Fig. 3). All the ratios were calculated from the major peak areas of NaMgCl₃ and Na₆MgCl₈. The low NaMgCl₃-to-Na₆MgCl₈ ratio in the rapid-quenched sample indicated that much more Na₆MgCl₈ was present than was expected according to the stoichiometric calculations. The drastic difference between the ratios with different cooling rates suggests that the molten phase is different than predicted by equilibrium.

Similarly to the studied NaCl:MgCl₂ mixture, the quenching method affected the phase composition of the binary KCl:MgCl₂ (68:32) mixture (Fig. 4). The most striking difference is the peak around 36.5 deg, which is notably higher in the rapidly cooled sample compared to the two other samples and corresponds to the [200] plane of K₂MgCl₄. Regarding other peaks, the diffractogram of the rapidly cooled sample differs from the diffractograms

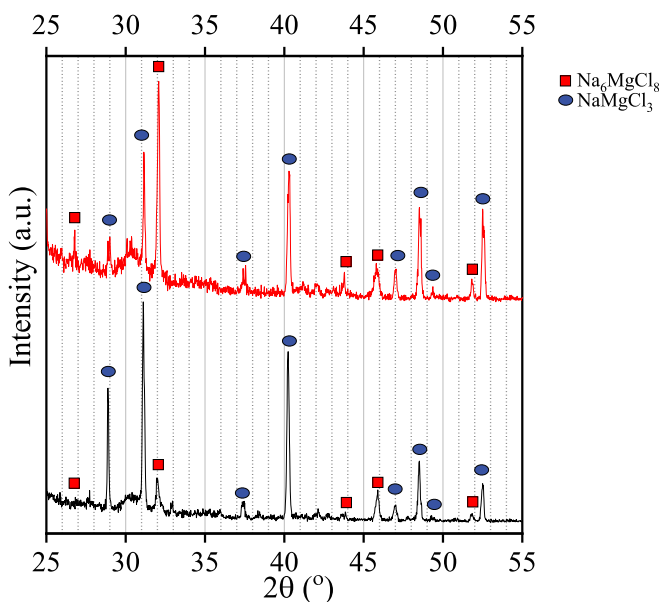


Fig. 3. X-ray diffraction patterns of rapidly quenched (top pattern) and splat-quenched (bottom pattern) NaCl:MgCl₂ salt. The small peaks at around 30 and 33 deg are from a plastic dome that was used to protect the salts from exposure to air.

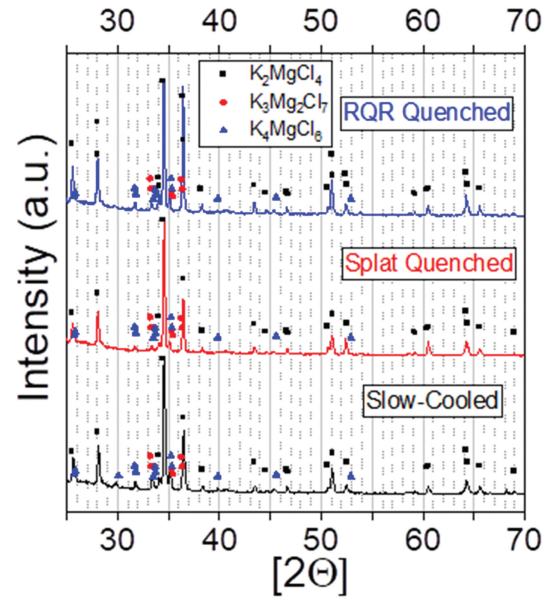


Fig. 4. X-ray diffraction patterns of rapidly quenched, splat-quenched, and slow-cooled KCl:MgCl₂ salt.

of the two splat-quenched and slow-cooled samples, which appear to be closer to one another. Another feature worth noticing is that the KCl:MgCl₂ (68:32) system is at the eutectic point, where the expected products/phases are K₂MgCl₄, K₃Mg₂Cl₇, and KMgCl₃ with melting points of 426°C, 440°C, and 488.5°C, respectively. However, no peaks for KMgCl₃ were identified, which could originate from a high enough cooling rate, which prevents structures with higher melting points from crystallizing. The cooling rate-dependent differences in the diffractograms provide further support for the applicability of the presented method in terms of rapid quenching of molten samples.

The XRD analysis of the mixed KCl:MgCl₂ + 5 wt% CrCl₃ sample identified only CrCl₃ and K₂MgCl₄, indicating isolated phases with unchanged structures (Fig. 5, upper diffractogram). When the same mixture was fused instead of being mixed, CrCl₃, K₃CrCl₆, and KMgCl₃ were identified (Fig. 5, lower diffractogram). The presence of CrCl₃ in the fused sample suggested that the solubility of CrCl₃ in a KCl:MgCl₂ salt was low since either it had not fully dissolved in the mixture or it did not remain dissolved. Based on phase diagrams, CrCl₆³⁻ was the principal Cr(III)-containing species, which explains the identification of K₃CrCl₆.^[26] Fusing CrCl₃ with KCl:MgCl₂ (68:32) changed the crystallized structure from predominantly K₂MgCl₄ to KMgCl₃. K₂MgCl₄ has been reported to be stable in the molten state but decomposed into KMgCl₃ and KCl during recrystallization.^[27] The fact

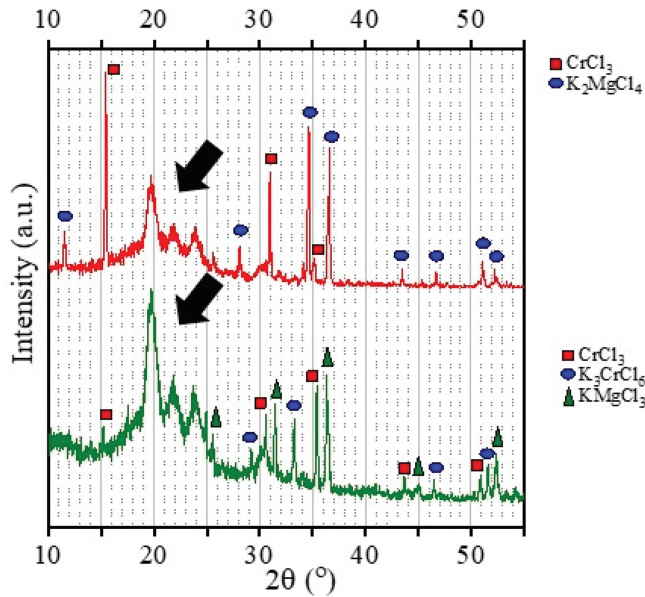


Fig. 5. The main diffractions of a mixed (top pattern) and fused (bottom pattern) KCl:MgCl₂+CrCl₃ salt. The arrows indicate the peaks from the plastic dome that was used to protect the salts from exposure to air.

that XRD captured and identified the change in the predominant structure suggests that the method could be used in the future to probe differences in the crystal structure of corrosion products in molten salts.

Unfortunately, no distinctive differences in identified phases between the slowly and the rapidly cooled KCl:MgCl₂+CrCl₃ samples were observed. For both samples, the XRD pattern was mainly identified with K₃Mg₂Cl₇

and K₂MgCl₄ phases followed by a smaller amount of CrCl₃. In both samples, some of the XRD peaks presented in Fig. 5 originate from the plastic dome that was used to protect the salts from exposure to air (indicated with black arrows). Further challenges for phase identification originate from the possibly small amount and peak mixing/overlapping of the additional phases.

III.C. Electron Paramagnetic Resonance

Electron paramagnetic resonance measures the response of unpaired electrons surrounding an atom. Transition metals are well suited for characterization with this technique, making EPR a promising candidate to study corrosion product structure in molten salts. As a first step to study the suitability of EPR to distinguish and identify chromium species dissolved in the molten salt, samples of CrCl₂, CrCl₃, and Cr₂O₃ were analyzed with EPR (Fig. 6). For CrCl₃, signals at 0.345 T (3450 G) and 0.357 T (3570 G) were observed, whereas no signals were detected for CrCl₂ (Fig. 6a). The signal positions for CrCl₃ agree well with previously reported measurements, and the lack of response in the case of CrCl₂ can be explained with the antiferromagnetic nature of the species.^[28] This feature can be used in the future to identify different oxidation states of chromium chlorides (CrCl_x). Cr₂O₃ is also antiferromagnetic and, thus, generated no signal in the EPR measurement (Fig. 6b). Interestingly, the transition of Cr₂O₃ to its paramagnetic form occurs at temperatures above

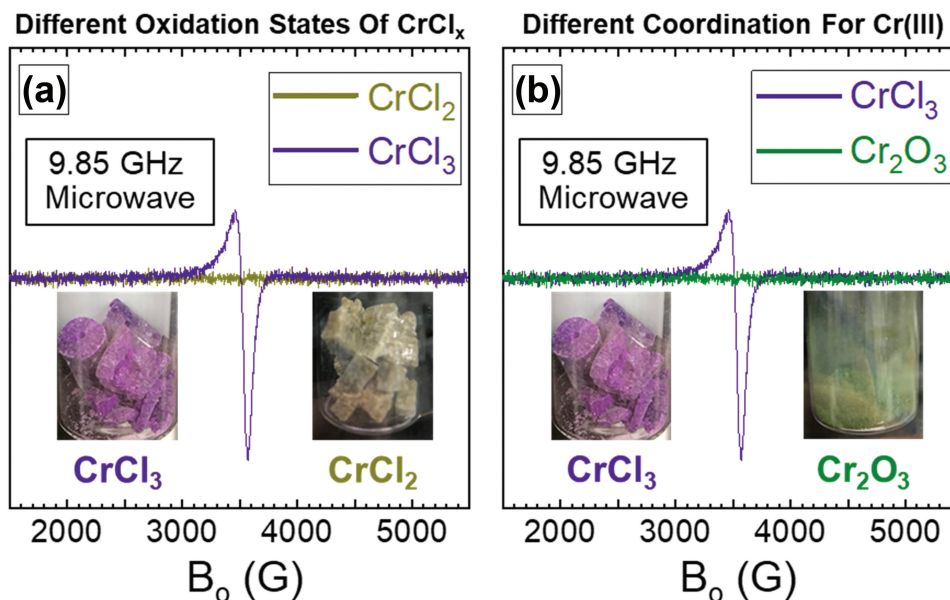


Fig. 6. The measured EPR signals for (a) CrCl_x species and (b) Cr(III) species.

37°C.^[29] This enables the identification of Cr₂O₃, and because of the temperature dependency of its magnetic nature, it can be distinguished from CrCl₂. Although not measured in this study, EPR has been reported to also identify more complex Cr-containing compounds such as KCrCl₃, K₂CrCl₄, K₃CrCl₆, and K₃Cr₂Cl₉.^[30] However, for a comprehensive understanding of the potential of EPR in molten salt corrosion studies, additional work is required regarding signal interpretation in complex chemical environments. Nevertheless, EPR appears to be a promising tool for molten salt chemistry research.

IV. CONCLUSIONS

The Rapid Quenching Reactor, a new design for rapid cooling and solidification of molten salt samples, was constructed, and its functionality was demonstrated with salt mixtures of industrial relevance. By melting the samples and rapidly introducing them into liquid argon, the design accelerates the cooling process and produces distinct and uniform samples of solid salt without introducing impurities.

Because of the direct introduction of the molten salt sample into liquid argon, the obtained cooling rates produced solid sample particles with sizes controllable by the carrier gas flow rate. In addition, the shielded structure of the apparatus prevented exposure of the rapidly quenched salt to impurities (humidity, oxygen, etc.), which would distort the results of the postexperimental characterization. XRD results revealed that quenching the salt in liquid argon produced structures in quantities further from stoichiometric equilibrium, which indicates the design produces resolidified salt with a kinetically favored structure. This suggests that the novel design solidifies salts in a way that may provide insight into the liquid chemical structure, although further work is needed to understand this aspect, especially for metallic impurities in the salt.

Disclosure Statement









No potential conflict of interest was reported by the author(s).

Funding

This work has been carried out within the Academy of Finland project “Initiation and Propagation of High-

Temperature Corrosion Reactions in Complex Oxygen-Containing Environments” (decision number 348963) and the Laboratory Directed Research and Development Program of Oak Ridge National Laboratory, managed by UT-Battelle, LLC, for the U.S. Department of Energy.

ORCID

Juho Lehmusto  <http://orcid.org/0000-0003-3495-4710>
 J. Matthew Kurley  <http://orcid.org/0000-0003-0592-0714>
 Ercan Cakmak  <http://orcid.org/0000-0001-7272-4815>
 James R. Keiser  <http://orcid.org/0000-0003-4718-7776>
 Daniel Lindberg  <http://orcid.org/0000-0002-4054-389X>
 Markus Engblom  <http://orcid.org/0000-0002-3100-9572>
 Bruce A. Pint  <http://orcid.org/0000-0002-9165-3335>
 Stephen S. Raiman  <http://orcid.org/0000-0002-4801-5098>

References

1. J. SERP et al., “The Molten Salt Reactor (MSR) in Generation IV: Overview and Perspectives,” *Prog. Nucl. Energy*, **77**, 308 (2014); <https://doi.org/10.1016/j.pnucene.2014.02.014>.
2. J. C. GOMEZ-VIDAL and R. TIRAWAT, “Corrosion of Alloys in a Chloride Molten Salt (NaCl-LiCl) for Solar Thermal Technologies,” *Sol. Energy Mater. Sol. Cells*, **157**, 234 (2016); <https://doi.org/10.1016/j.solmat.2016.05.052>.
3. A. HOSHI et al., “Screening of High Melting Point Phase Change Materials (PCM) in Solar Thermal Concentrating Technology Based on CLFR,” *Sol. Energy*, **79**, 3, 332 (2005); <https://doi.org/10.1016/j.solener.2004.04.023>.
4. A. FERRARA, R. HASLETT, and J. JOYCE, “Molten Salt Thermal Energy Storage for Utility Peaking Loads,” *Proc. 12th Intersociety Energy Conversion Engineering Conference*, 1977, p. 547.
5. D. F. WILLIAMS, “Assessment of Candidate Molten Salt Coolants for the NNGP/NHI Heat-Transfer Loop,” ORNL/TM-2006/69, Oak Ridge National Laboratory (2006).
6. Y. HOSOYA et al., “Compatibility of Structural Materials with Molten Chloride Mixture at High Temperature,” *J. Nucl. Mater.*, **248**, 348 (1997); [https://doi.org/10.1016/S0022-3115\(97\)00175-X](https://doi.org/10.1016/S0022-3115(97)00175-X).
7. J. E. INDACOCHEA et al., “High Temperature Oxidation and Corrosion of Structural Materials in Molten Chloride Salts,” *Oxid. Met.*, **55**, 1–2, 1 (2001); <https://doi.org/10.1023/A:1010333407304>.

8. T. ISHITSUKA and K. NOSE, "Stability of Protective Oxide Films in Waste Incineration Environment—Solubility Measurement of Oxides in Molten Chloride," *Corros. Sci.*, **44**, 2, 247 (2002); [https://doi.org/10.1016/S0010-938X\(01\)00059-2](https://doi.org/10.1016/S0010-938X(01)00059-2).
9. J. M. KURLEY et al., "Enabling Chloride Salts for Thermal Energy Storage: Implications of Salt Purity," *RSC Adv.*, **9**, 44, 25602 (2019); <https://doi.org/10.1039/C9RA03133B>.
10. B. A. PINT et al., "Reestablishing the Paradigm for Evaluating Halide Salt Compatibility to Study Commercial Chloride Salts at 600°-800°C," *Mater. Corros.*, **70**, 1439 (2019); <https://doi.org/10.1002/maco.201810638>.
11. M. ŠIMURDA et al., "Analysis of the Extremely Rapidly Cooled Molten System (LiF-CaF₂)_{eut}-LaF₃," *New J. Chem.*, **42**, 6, 4612 (2018); <https://doi.org/10.1039/C7NJ05156E>.
12. S. GUO et al., "Measurement of Europium (III)/Europium (II) Couple in Fluoride Molten Salt for Redox Control in a Molten Salt Reactor Concept," *J. Nucl. Mater.*, **496**, 197 (2017); <https://doi.org/10.1016/j.jnucmat.2017.09.027>.
13. L. SANG et al., "Mixed Metal Carbonates/Hydroxides for Concentrating Solar Power Analyzed with DSC and XRD," *Sol. Energy Mater. Sol. Cells*, **140**, 167 (2015); <https://doi.org/10.1016/j.solmat.2015.04.006>.
14. A.-L. BIANCE, C. CLANET, and D. QUERE, "Leidenfrost Drops," *Phys. Fluids*, **15**, 1632 (2003).
15. H. HONDA, O. MAKISHI, and H. YAMASHIRO, "Generalized Stability Theory of Vapor Film in Subcooled Film Boiling on a Sphere," *Int. J. Heat Mass Transfer*, **50**, 17-18, 3390 (2007); <https://doi.org/10.1016/j.ijheatmasstransfer.2007.01.043>.
16. Z. XU and Y. ZHANG, "Quench Rates in Air, Water, and Liquid Nitrogen, and Inference of Temperature in Volcanic Eruption Columns," *Earth Planet. Sci. Lett.*, **200**, 315 (2002); [https://doi.org/10.1016/S0012-821X\(02\)00656-8](https://doi.org/10.1016/S0012-821X(02)00656-8).
17. O. MENGE, "Die binären Systeme von MgCl₂ und CaCl₂ mit den Chloriden der Metalle K, Na, Ag, Pb, Cu', Zn, Sn' und Cd," *Z. Anorg. Allg. Chem.*, **72**, 162 (1911); <https://doi.org/10.1002/zaac.19110720113>.
18. S. POLIMENI et al., "Comparison of Sodium and KCl-MgCl₂ as Heat Transfer Fluids in CSP Solar Tower with sCO₂ Power Cycles," *Sol. Energy*, **162**, 510 (2018); <https://doi.org/10.1016/j.solener.2018.01.046>.
19. X. XU et al., "Experimental Test of Properties of KCl-MgCl₂ Eutectic Molten Salt for Heat Transfer and Thermal Storage Fluid in Concentrated Solar Power Systems," *J. Sol. Energy Eng.*, **140**, 5, 051011 (2018); <https://doi.org/10.1115/1.4040065>.
20. C. W. BALE et al., "FactSage Thermochemical Software and Databases, 2010–2016," *Calphad*, **54**, 35 (2016); <https://doi.org/10.1016/j.calphad.2016.05.002>.
21. J. C. ARD et al., "Thermodynamic Assessments or Reassessments of 30 Pseudo-Binary and -Ternary Salt Systems," *J. Chem. Thermodyn.*, **177**, 106931 (2023); <https://doi.org/10.1016/j.jct.2022.106931>.
22. A. D. PELTON and P. CHARTRAND, "Thermodynamic Evaluation and Optimization of the LiCl-NaCl-KCl-RbCl-CsCl-MgCl₂-CaCl₂ System Using the Modified Quasi-Chemical Model," *Metall. Mater. Trans. A*, **32**, 1361 (2001); <https://doi.org/10.1007/s11661-001-0227-2>.
23. H.-J. SEIFERT and G. THIEL, "Lösungskalorimetrische Messungen an Doppelchloriden des Magnesiums," *Z. Anorg. Allg. Chem.*, **436**, 237 (1977); <https://doi.org/10.1002/zaac.19774360131>.
24. Jade 2010 (computer software), Materials Data Inc. (2010).
25. PDF-4+ 2019, International Centre for Diffraction Data (2019).
26. C. M. COOK Jr., "The Systems NaCl-CrCl₃ and NaCl-CrCl₃," *J. Inorg. Nucl. Chem.*, **25**, 1, 123 (1963); [https://doi.org/10.1016/0022-1902\(63\)80218-3](https://doi.org/10.1016/0022-1902(63)80218-3).
27. B. F. MARKOV, T. A. TISHURA, and A. N. BUDARINA, "Thermochemical Study of Binary Salt Systems," *Rev. Roum. Chim.*, **20**, 5, 597 (1975).
28. G. L. MCPHERSON and K. O. DEVANEY, "EPR Spectra of Chromium⁽³⁺⁾ and Chromium⁽¹⁺⁾ Centers in the Linear-Chain Lattices, CsMgCl₃, CsMgBr₃ and CsCdBr₃," *J. Phys. C: Solid State Phys.*, **13**, 9, 1735 (1980); <https://doi.org/10.1088/0022-3719/13/9/019>.
29. V. G. ANUFRIEV, "EPR of Cr₂O₃ in the Phase Transition Region," *Phys. Lett.*, **64A**, 1, 139 (1977); [https://doi.org/10.1016/0375-9601\(77\)90556-4](https://doi.org/10.1016/0375-9601(77)90556-4).
30. D. H. LEECH and D. J. MACHIN, "Preparation and Magnetic Properties of Alkali Metal Salts of Chlorochromate(II) and Chlorochromate(III) Anions," *J. Chem. Soc., Dalton Trans.*, **15**, 1609 (1975); <https://doi.org/10.1039/dt9750001609>.